Paper Number: 093

CFD Prediction of Air Flow Past a Full Helicopter Configuration

Walid Khier[1], Massimo Biava[2] and Luigi Vigevano[3]

[1] Institut für Aerodynamik und Strömungstechnik,
Deutsches Zentrum für Luft- und Raumfahrt e.V. (DLR)
Lilienthalplatz 7, 38108 Braunschweig, Germany
email: walid.khier@dlr.de

[2] AgustaWestland-Politecnico Advanced Rotorcraft Center S.r.l. (AWPARC)
Via Durando Giovanni 10, 20158 Milan, Italy

[3] Dipartimento di Ingegneria Aerospaziale, Politecnico di Milano
Via La Masa 34, 20156 Milan, Italy

ABSTRACT

In this paper the numerical results of two GOAHEAD partners, the German Aerospace Center (DLR) and Politecnico di Milano (PoliMi) are presented and compared to experimental measurements. The paper also addresses an evaluation of two different approaches to predict helicopter flows. The first, applied by DLR, accounts for rotor trim and elastic effects by weak fluid-structure coupling. The PoliMi approach, on the other hand, enforces a prescribed kinematics obtained either by applying the comprehensive code HOST, or taken directly from the experiment. The computational model refers to a wind tunnel complete helicopter model, featuring a 4.1 m NH90 fuselage model, ONERA 7AD main rotor, reduced scale BO105 tail rotor, a rotor hub, a strut and slip ring fairing inside the 8m x 6m test section of the DNW low-speed wind tunnel. The flight conditions correspond to cruise flight at Ma=0.204 and fuselage attitude α=-2.5°. The comparisons demonstrate the capability of unsteady RANS solvers to predict flow fields around helicopters.

INTRODUCTION

Computational Fluid Dynamics (CFD) has evolved as a prediction tool in helicopter research and development field over the past two decades. Application of CFD to the individual components of the aircraft, such as the fuselage and the rotor, was carried out successfully demonstrating the usefulness of CFD in the early design phase of the aircraft.

Although the capabilities of CFD tools to predict the flow past a complete helicopter have been shown ([1] and [2]), they could not be thoroughly validated for this class of flows due to the lack of suitable experimental database.

Impelled by the industrial need for reliable tools to predict the aerodynamic characteristics of the complete aircraft, a consortium of leading research institutes and helicopter manufacturers initiated the EU project GOAHEAD, [3]-[4], in 2005. The main objectives of the project are to create an experimental database for the validation of CFD codes in helicopter related applications, and to apply this database to validate modern CFD tools. The measurements were successfully carried out at the German-Dutch low speed wind tunnel (DNW) in spring 2008. The GOAHEAD test campaign included detailed steady and unsteady surface pressure measurements on the helicopter and tunnel walls, transition locations, inflow velocity and turbulence kinetic energy levels and PIV measurements for a wide array of flight and rotor loading conditions. A code validation activity was carried out separately within the project. The blind validation computations were documented in [5] and [6] and were compared to the measurements in [7].

Numerical simulation of a complete helicopter is a very demanding process. Not only does it involve intensive computational resources but requires advanced CFD functionalities as well. To predict the flowfield around a helicopter by a specific solver, it must be able to tackle flow unsteadiness, multiple relative motions and, depending on the simulation approach, surface and volume grid deformation.

Elastic deformation of loaded helicopter main rotor blades is undoubtedly a major factor affecting the performance of the rotor. Torsional, flapping and lead-lag oscillations alter the direction of the flow relative to the blade, leading to a deviation in rotor forces with respect to its performance under rigid

blade assumption [8]. There have been two main approaches to include blade elasticity: weak (or loose) coupling or strong coupling with a flight and structural mechanics tool. However, both options increase the complexity and computational costs considerably.

Obviously, the significance of fluid-structure coupling increases as the stiffness of the blades decreases. For moderately loaded stiff blades, it is not clear how far elastic effects may affect the accuracy of the numerical predictions, and whether these differences justify the additional computational overhead.

In this paper the contributions of DLR and PoliMi to the post test validation activity of GOAHEAD are reported. The numerical predictions are judged against the GOAHEAD experimental database to asses the ability and accuracy of DLR and PoliMi RANS solvers to predict the complex flow phenomena related to helicopters. The effect of elastic deformation on the stiff ONERA 7AD blade is also assessed by comparison of two different simulation approaches: weak fluid-structure coupling to trim the rotor, which was applied by DLR, and that of PoliMi where the blade motion and deformation were directly taken from the experiment.

The computational model and flow conditions are described in the next part. The numerical approach and computational grid are presented in the subsequent parts. The fifth part of the paper is dedicated to the numerical results and their comparison with the experimental data. Finally, the conclusions are listed in the sixth and last section of this paper.

COMPUTATIONAL MODEL AND FLOW CONDITIONS

The computational model refers to the GOAHEAD wind tunnel model (Figure 1). It consists of a 4.1 m NH90 fuselage model, ONERA 7AD main rotor, reduced scale BO105 tail rotor, a main rotor hub, a strut and slip ring fairing and 8m x 6m test section of 20m length. Both the main and tail rotors are represented by isolated blades. The main rotor hub is simplified to a cylindrical element and an elliptical hub fairing. The tail rotor hub is not included in the computational model. Forward flight condition at Mach number equal 0.204 and -2.5° fuselage pitch angle was considered.

APPROACH

The numerical approach employed in this paper is based on the solution of the Reynolds (Favre) averaged Navier-Stokes equations in three dimensions accurately in time by means of the CFD

block-structured, finite volume code FLOWer ([10]-[11]), on the DLR side while PoliMi applied the in house developed code ROSITA [16].

FLOWer contains a large array of statistical turbulence models, ranging from algebraic and one-equation eddy viscosity models (Refs [12]-[13]) to seven-equation Reynolds stress model. In this paper a slightly modified version ([14]) of Wilcox's two-equation k-ω model [15] is used. Unlike the main flow equations, Roe's scheme is employed to compute the turbulent convective fluxes.

The ROSITA code is based on the multi-block and finite volume approach coupled with the one-equation Spalart-Allmaras model to achieve the closure of the RANS equations. Flow problems involving motion or complex geometry can be treated via overset systems of moving multi-block grids. Roe scheme is used for the convective fluxes with a MUSCL extrapolation combined with a modified version of the Van Albada limiter introduced by Venkatakrishnan [17] to ensure second order accuracy. Central difference is used to discretize the viscous terms while time advancement is carried out with a dual time approach employing a second order backward differentiation formula.

Both codes rely on a moving Chimera technique to introduce the motion of the blades in the simulation process. The implementation of Chimera in FLOWer follows the ideas of Benek [18]. PoliMi's approach is derived from that originally proposed by Chesshire and Henshaw [19] with modifications to improve robustness and performance. For integration of the aerodynamic forces on overlapping surface grids, a special treatment proposed by Chan and Buning [20] is used.

The rotor was trimmed using the stand alone flight mechanics tool HOST (Helicopter Overall Simulation Tool) to generate the experimental weight, lateral and propulsive force coefficients in the DLR computations. The resulting rotor controls and elastic deformation were used to modify the blade surface geometry following the approach presented in [21]-[23]. The process is described in detail in [6] and [24]. PoliMi's simulation featured a rigid rotor with experimental input for blade pitch, flap and lead-lag commands.

NUMERICAL GRID

Multi-block grids around the different elements were subdivided into 10 Chimera components: fuselage, rotor hub, four main rotor blades, two tail rotor blades, model strut and wind tunnel walls. Figure 2 shows the surface grid for the complete helicopter configuration, while Table 1 lists the major characteristics of the numerical grids used.

No. of points (x10^6)	PoliMi	DLR
Fuselage	17.4	18.1
Main rotor blade (x 4)	1	0.87
Tail rotor blade (x 2)	0.5	0.35
Rotor hub	2	2.12
Strut	1.3	0.9
Wind tunnel	1.3	0.3
Total (Mil. point)	27	25.6

Table 1: Summary of DLR and PoliMi Grid parameters

RESULTS

The fuselage is equipped with a total number of 130 unsteady pressure sensors. Figure 3 compares the computed pressure signals with the experiment for selected 12 sensors. It should be noted that the main rotor rotates in clockwise direction as seen from above. The upper vertical tail rotor blade is advancing and the lower vertical blade is retreating.

Strong oscillations were found in the experimental pressure [7], which were most probably due to vibration of the model inside the tunnel. The experimental data shown in the figure were obtained by averaging the pressure signals recorded for each azimuthal position over 130 revolutions.

Broadly good agreement between measurements and computations can be observed for the sensors on the nose (Figure 3.a) and on the windscreen (Figure 3.b and c). The influence of the rotor is well captured in the computations in terms of frequency and phase. PoliMi results show slight underestimation of pressure on the nose and the advancing blade side. Both sets of CFD results predict higher pressure values on the retreating side (Figure 3.c). Computed pressure signals on the upper side of the tail boom are characterized by high frequency oscillation especially on the advancing blade side as seen in Figure 3.d and c. The average value is well predicted by DLR and PoliMi. High frequency oscillations are observed also on the lower side of the tail boom. PoliMi results are closer to the experiment on the advancing side as shown Figure 3.f but with strong overshoots of the peak values, while DLR results follow the experimental trend but at a nearly constant offset. As far as the average values are concerned, the agreement becomes better on the retreating side (Figure 3.g). The effect of the main rotor cannot be easily identified in the tail fin signals depicted in Figure 3.h and Figure 3.i probably due to strong interference between the fuselage and main rotor wakes with the tail rotor and tail fin. DLR results show however an evident 4/Rev pattern. PoliMi data is dominated by high frequency oscillation but remains close to the measurements. Figure 3.j-l contains the pressure data on the advancing side (Figure 3.j) back door,

symmetry plane (Figure 3.k) and the retreating side (Figure 3.l) of the back door. Inspection of measured data reveals slight decrease in average pressure from the advancing side towards the retreating side (Figure 3.j to l). Pressure pulses are observed on the advancing side sensor indicating influence of the rotor on the flow in this region. The amplitude of signal vanishes almost completely as the symmetry plane is approached before it increases slightly on the retreating side. A similar behaviour cannot be observed in the numerical data. DLR and PoliMi predictions overestimate the pressure and do not show harmonic evolution with the azimuth angle.

Snapshots of surface pressure at symmetry plane are illustrated in Figure 4. Accurate prediction of the rapid pressure drop on the leading end of the fuselage and the subsequent pressure recovery downstream the mast fairing can be clearly seen in the figure. DLR and PoliMi results show similar level of accuracy except in the nose and wind shield areas where the DLR results are slightly closer to the experimental data. The pressure recovery zone downstream the mast fairing is another area where differences in the numerical data can be seen. The differences between the numerical results are however small.

Computed and measured pressure coefficients on the main rotor blade are compared in Figure 5 to Figure 7. The figures respectively show the pressure at selected radial positions: r/R=0.500, 0.825 and 0.975 for one main rotor revolution at azimuthal spacing of 30°. Experimental values are represented by symbols while the numerical results are represented by solid curves. The pressure sensors were distributed on three blades. For each blade a different colour is used in the figures. The experimental data shown were averaged over a comparably large number of rotor revolutions of that used for the fuselage sensors.

Qualitatively, the computations captured the pressure pattern well over the whole revolution for the three radial locations. PoliMi pressure values are generally higher than the DLR pressure on the suction side (Figure 5).

At r/R=0.825, Figure 6, the computational results are very close to the experimental data. Apart from discrepancy on the suction side in the range Ψ=30° to 90°, and at Ψ=150°, the numerical results match the measurements very good.

Similarly good agreement is found in Figure 7 for the radial location r/R=0.975. A reduction in the advancing range discrepancy found in Figure 6 is observed. The differences between DLR and PoliMi results diminish with radial distance where the largest differences between the two approaches are expected. The elastic effects were most probably

compensated in PoliMi's trim procedure by a different pitch and flap combination, which lead finally to a similar local pitch angle.

Tail rotor pressures at the radial locations r/R= 0.97 are presented respectively in Figure 8. Similar to the main rotor data, sectional pressure plots are shown with azimuthal spacing of 30°. Solid curves refer to numerical results and symbols refer to measured data. DLR computations were performed using the experimental pitch values while the commands for the flap motion were taken from the blind test matrix. This obviously impaired the accuracy of predictions below the level of the blind test computations reported in [7]. On the other hand, PoliMi adopted the experimental values for both pitch and flap control angles, but this did not lead to a noticeable better agreement with the experimental data.

	Percentage of experiment (%)
Coupled simulation (DLR)	99.76
Rigid blade (PoliMi)	85

Table 2: Main rotor power consumption

Main rotor power consumption values are listed in Table 2. Rigid blade assumption clearly underestimates power consumption. Fluid-structure coupling considerably improves the power prediction with an error of 0.24% only.

CONCLUSIONS

Results of the final DLR and PoliMi GOAHEAD simulation were examined by comparison with experimental data. Weak fluid-structure coupling was iteratively applied by DLR to trim the main rotor while PoliMi applied the experimental rotor controls.

Good agreement between computed and measured pressure signals on the front upper part of the fuselage in terms of phase and magnitude could be found. On the tail boom and tail gate evident discrepancy was observed. Both CFD approaches predicted fuselage surface pressure with similar accuracy indicating negligible influence of the modelling approach on the fuselage.

As to be expected, the most obvious discrepancy between DLR and PoliMi was found on the main rotor. However, the observed differences decreased rapidly in the direction of the blade tip.

The lack of accurate description of the tail rotor motion resulted in an evident mismatch between the CFD results and the experimental data.

Fluid-structure-flight mechanics coupling is an essential approach for accurate prediction of main rotor power. Coupled simulation predicted the power with an accuracy of 0.24%, while rigid blade assumption predicted 15% less power.

References

[1] W. Khier, F. Le Chuiton, T. Schwarz, Navier-Stokes Analysis of the Helicopter Rotor-Fuselage Interference in Forward Flight, CEAS Aerospace Aerodynamics Research Conference, 10-12 June 2002, Cambridge, England.

[2] Khier, W., Schwarz, T., Raddatz, J., Time Accurate Simlation Of The Flow Around The Complete BO105 Wind Tunnel Model, Proceedings of the 31st European Rotor Craft Forum, 13-15th Sept. 2005, Florence, Italy.

[3] Deutsches Zentrum für Luft- und Raumfahrt e.V. DLR, Generation of advanced helicopter experimental aerodynamic database for CFD code validation – GOAHEAD – Contract Nr. 516074: Annex I – Description of Work, November 2005.

[4] Pahlke, K., The GOAHEAD project, *Proceedings of the 33rd European Rotorcraft Forum*, Kazan, Russia, September 2007.

[5] Boelens, O.J., *et. al.*, The blind-test activity of the GOAHEAD project. *Proceedings of the 33rd European Rotorcraft Forum, Kazan, Russia,* September 2007.

[6] Khier, W., Dietz, M., Schwarz, T., and Wagner, S., Trimmed CFD Simulation of a Complete Helicopter Configuration*, Proceedings of the 33rd European Rotorcraft Forum, Kazan, Russia,* September 2007.

[7] Khier, W., Numerical Simulation of Air Flow Past a full Helicopter Configuration, *Proceedings of the 35th European Rotorcraft Forum*, Hamburg, Germany, September 2009.

[8] Pahlke, K., Van der Wall, B., Calculation of multi-bladed rotors in high speed forward flight

[9] Benoit, B., Dequin, A-M., Kampa, K., Grünhagen, W. v., Basset, P-M., Gimonet, B., HOST: A General Helicopter Simulation Tool for Germany and France. *56th Annual Forum of the American Helicopter Society, Virginia Beach, Virginia,* May 2000.

[10] Kroll, N., Rossow, C.-C., Becker, K., Thiele, F., The MEGAFLOW project, Aerospace, Science and Technology, Vol. 4, pp. 223-237, 2000.

[11] Kroll, N., Eisfeld, B., Bleecke, H.M., The Navier-Stokes Code FLOWer. Volume 71 of Notes on Numerical Fluid Mechanics, pp. 58-71. Vieweg, Braunschweig, 1999.

[12] Baldwin, B. S., Lomax, H., Thin Layeer Approximation and Algebraic Model for Separated Turbulent Flows, 78-0257, 1978.

[13] P. R. Spalart, S. R. Allmaras, A One-Equation Turbulence Model for Aerodynamic Flows, AIAA paper, 92-439, 1992.

[14] Rudnik, R., Untersuchung der Leistungsfähigkeit von Zweigleichungs-Turbulenzmodellen bei Profilumströmungen, Deutsches Zentrum für Luft- und Raumfahrt e.V., FB 97-49

[15] Wilcox, D. C., Reassessment of the Scale-Determining Equation for Advanced Turbulence Models, AIAA Journal, vol. 26, no. 11, November 1988.

[16] M. Biava, A. Pisoni, A. Saporiti, L. Vigevano, Efficient rotor aerodynamics predictions with an Euler method, 29th European Rotorcraft Forum, Friedrichshafen, Germany, 16-18 September 2003.

[17] Venkatakrishnan V., On the accuracy of limiters and convergence to steady state solutions, 31st AIAA Aerospace Sciences Meeting and Exhibit}, AIAA 93-0880, Reno, Nevada, 1993.

[18] Benek, J. A., Steger, J. L., Doughertz, F. C., A Flexible grid embedding technique with application to the Euler equations, AIAA Paper 83-1944.

[19] G. Chesshire and W. D. Henshaw, Composite overlapping meshes for the solution of partial differential equations, J. Comp. Phys., **90**, pp. 1--64, 1990

[20] W. M. Chan and P. G. Buning, Zipper grids for force and moment computation on overset grids, AIAA Paper 95-1681-CP

[21] Dietz, M., Krämer, E., Wagner, S., Altmikus, A., Weak coupling for active advanced rotors. *Proceedings of the 31st European Rotorcraft Forum, Florence, Italy,* September 2005.

[22] Dietz, M., Keßler, M., Krämer, E., Trimmed simulation of a complete helicopter configuration using fluid-structure coupling, to be published in high performance computing in science and engineering 2007, Springer Verlag, 2007.a.

[23] Dietz, M., Simulation der Umströmung von Hubschrauberkonfigurationen unter Berück-sichtigung von Strömung-Struktur-Kopplung und Trimmung. Ph.D. Thesis. Institut für Aerodynamik und Gasdynamik, Universität Stuttgart. Stuttgart, Germany, 2009.

[24] Dietz, M., Khier, W., Wagner, S. and Krämer, E., Numerical simulation of a full helicopter configuration using weak fluid-structure coupling. 46th AIAA Aerospace Sciences Meeting and Exhibit, Reno, Nevada, 7th–10th January 2008, AIAA 2008-401.
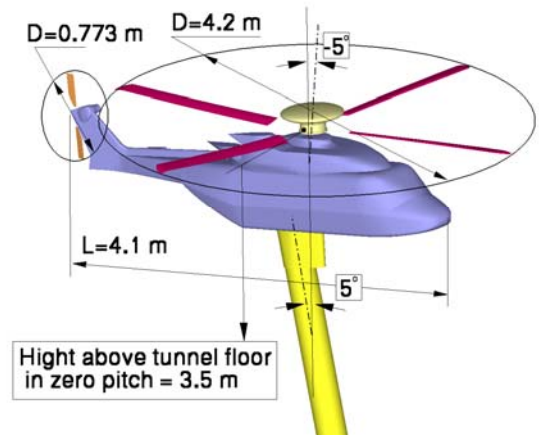
Figure 1: Left: Front view of the GOAHEAD model and experimental setup inside the wind tunnel. Right: Overview of the computational model showing its main components. Wind tunnel section not shown.
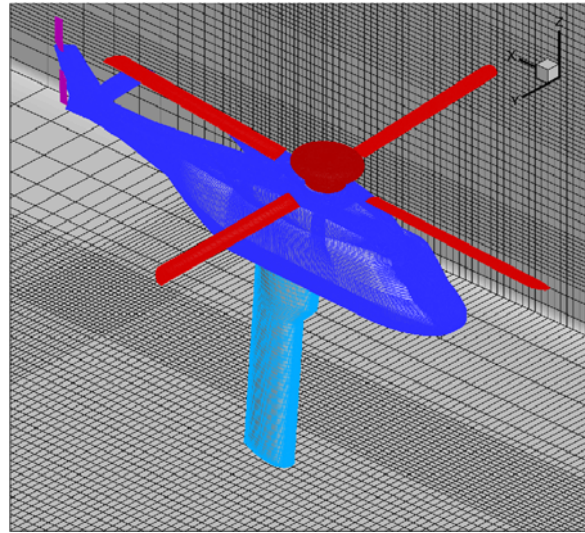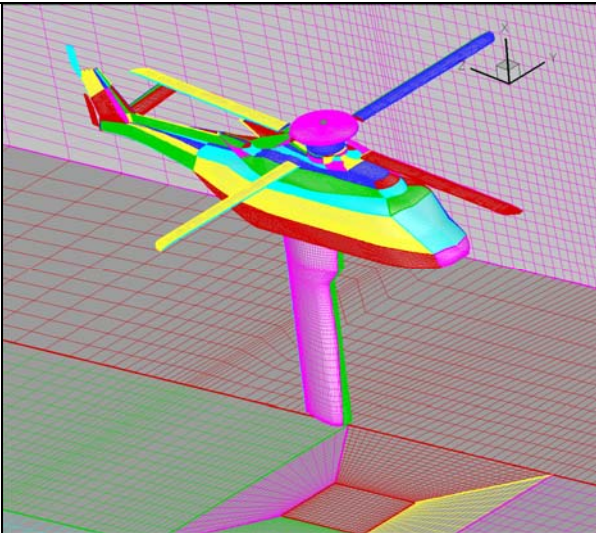

Figure 2: Surface grid on the model and wind tunnel walls. Left: DLR grid, Right: PoliMi grid.
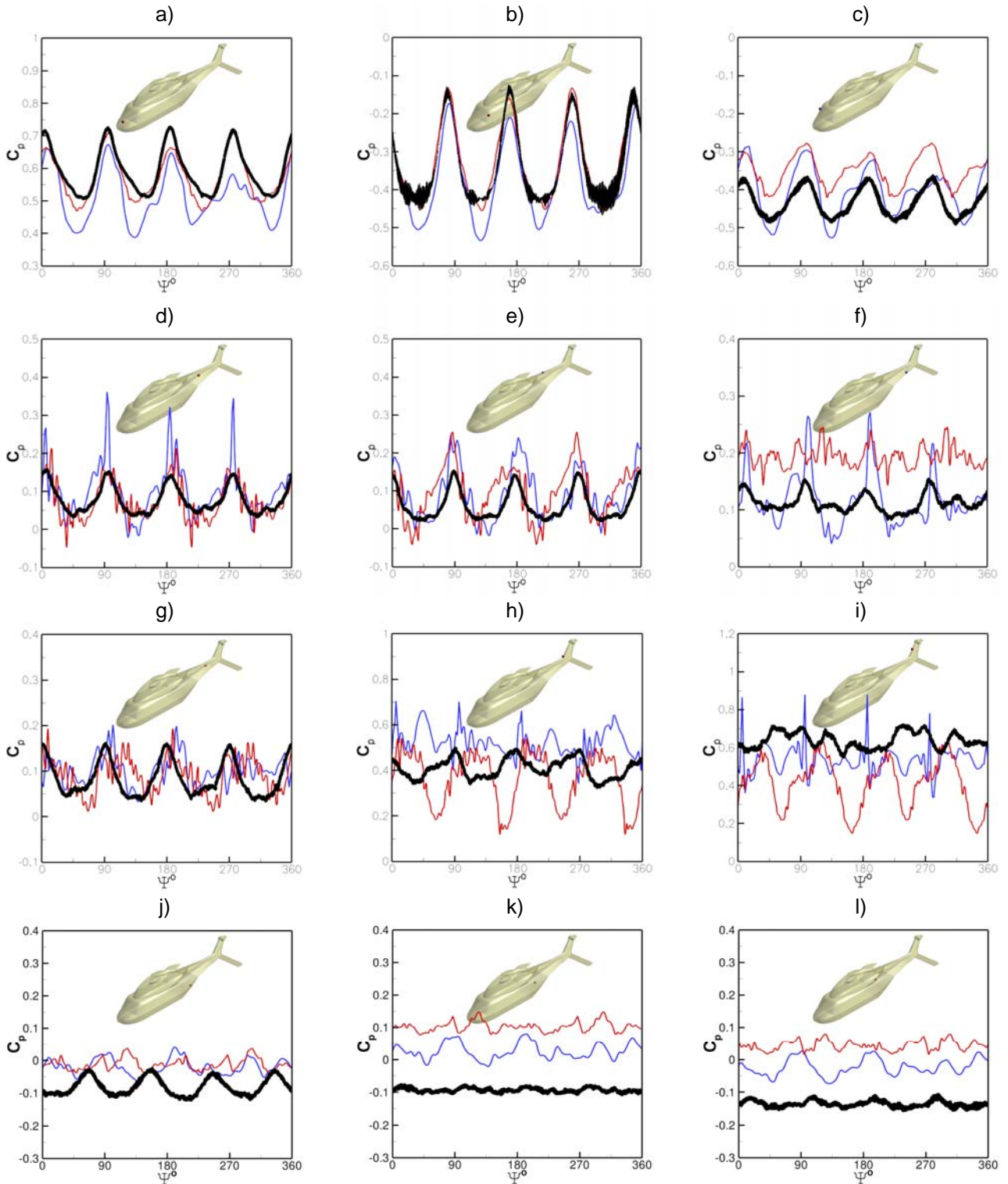
Figure 3: Evolution of computed and measured pressure signals at selected locations on the fuselage – M=0.204, $\theta_{fuselage}$=-2.5^o.. Red curves: DLR. Blue curves: PoliMi. Symbols: experiment.
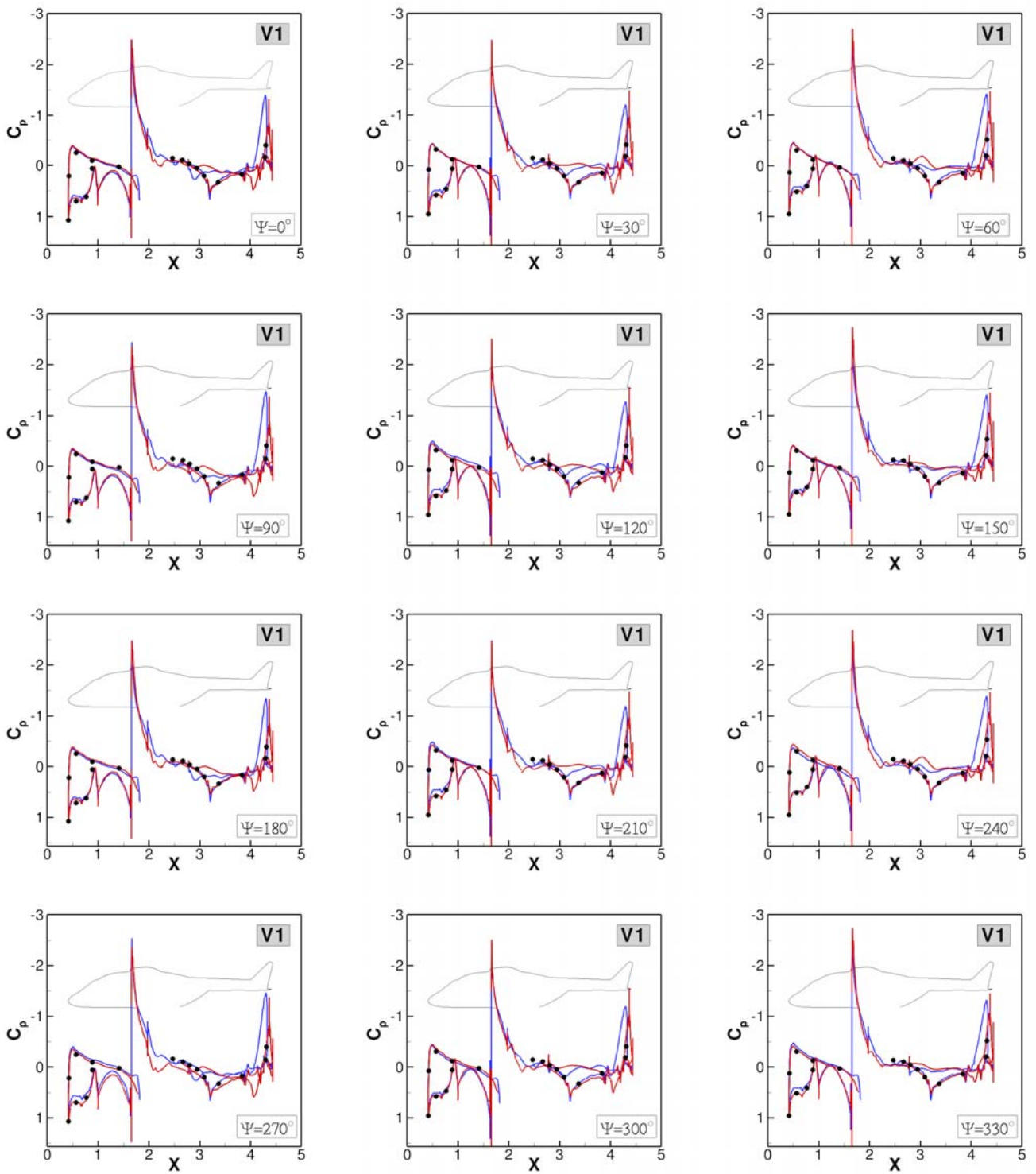
Figure 4: Comparison of computed and measured surface pressure coefficient at symmetry plane – M=0.204, $\theta_{fuselage}$=-2.5^{o}.. Red curves: DLR. Blue curves: PoliMi. Symbols: experiment.
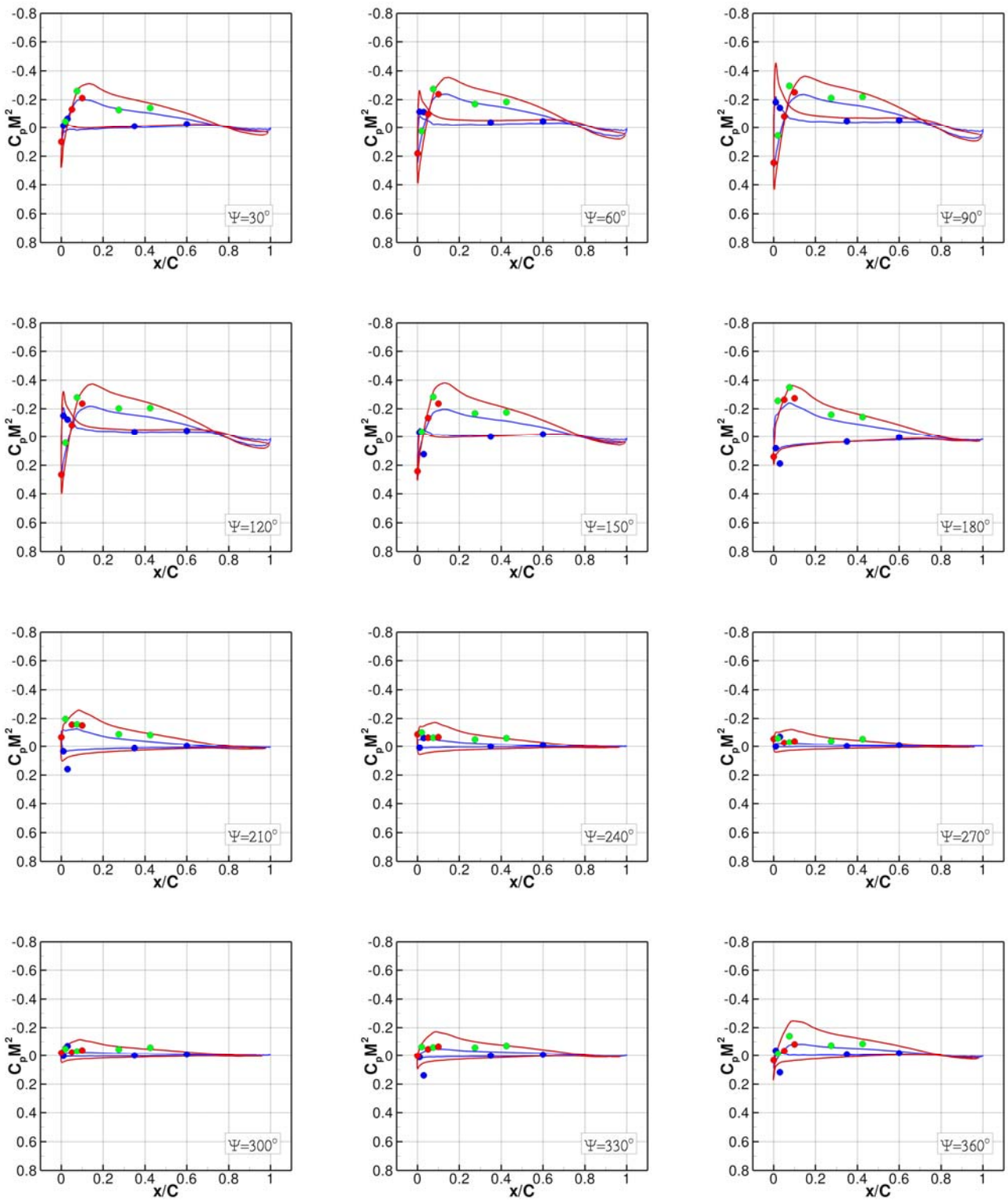
Figure 5: Computed and measured main rotor sectional pressure at r/R=0.500 over a complete revolution. Red curves: DLR. Blue curves: PoliMi. Symbols: experiment. Symbols of different colours denote different blades.
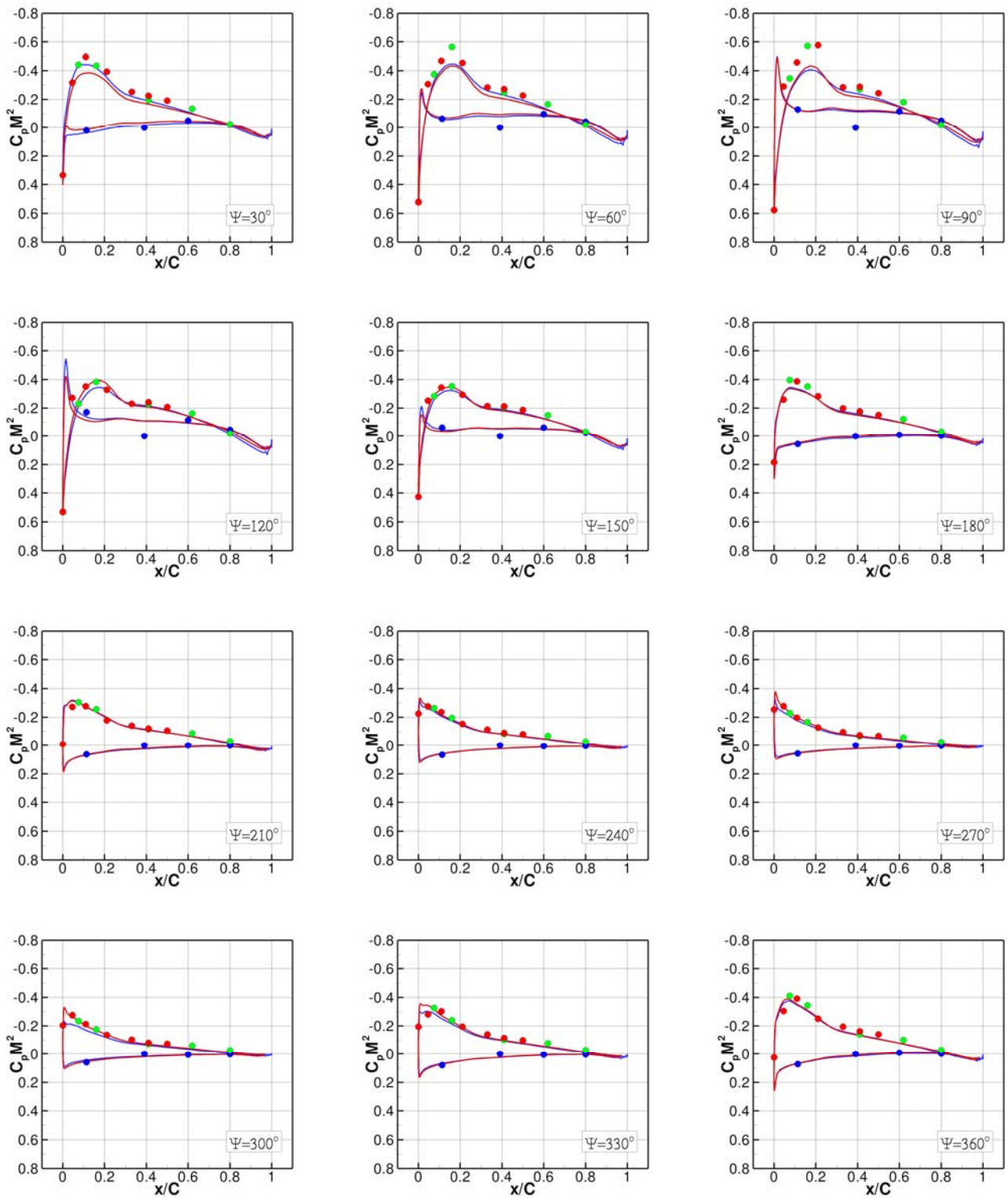
Figure 6: Computed and measured main rotor sectional pressure at r/R=0.825 at over a complete revolution. Red curves: DLR. Blue curves: PoliMi. Symbols: experiment. Symbols of different colours denote different blades.
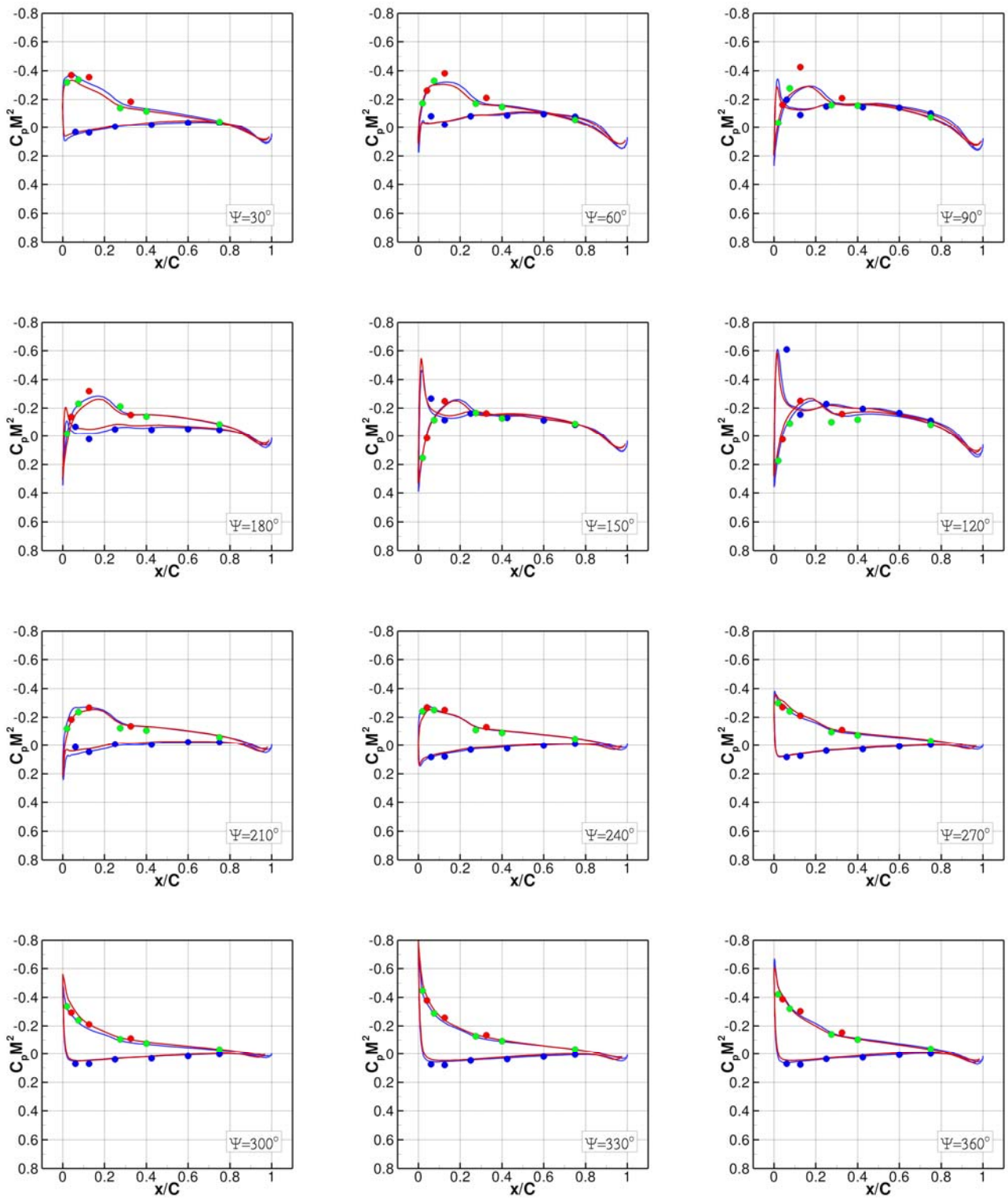
Figure 7: Computed and measured main rotor sectional pressure at r/R=0.975 over a complete revolution. Red curves: DLR. Blue curves: PoliMi. Symbols: experiment. Symbols of different colours denote different blades.
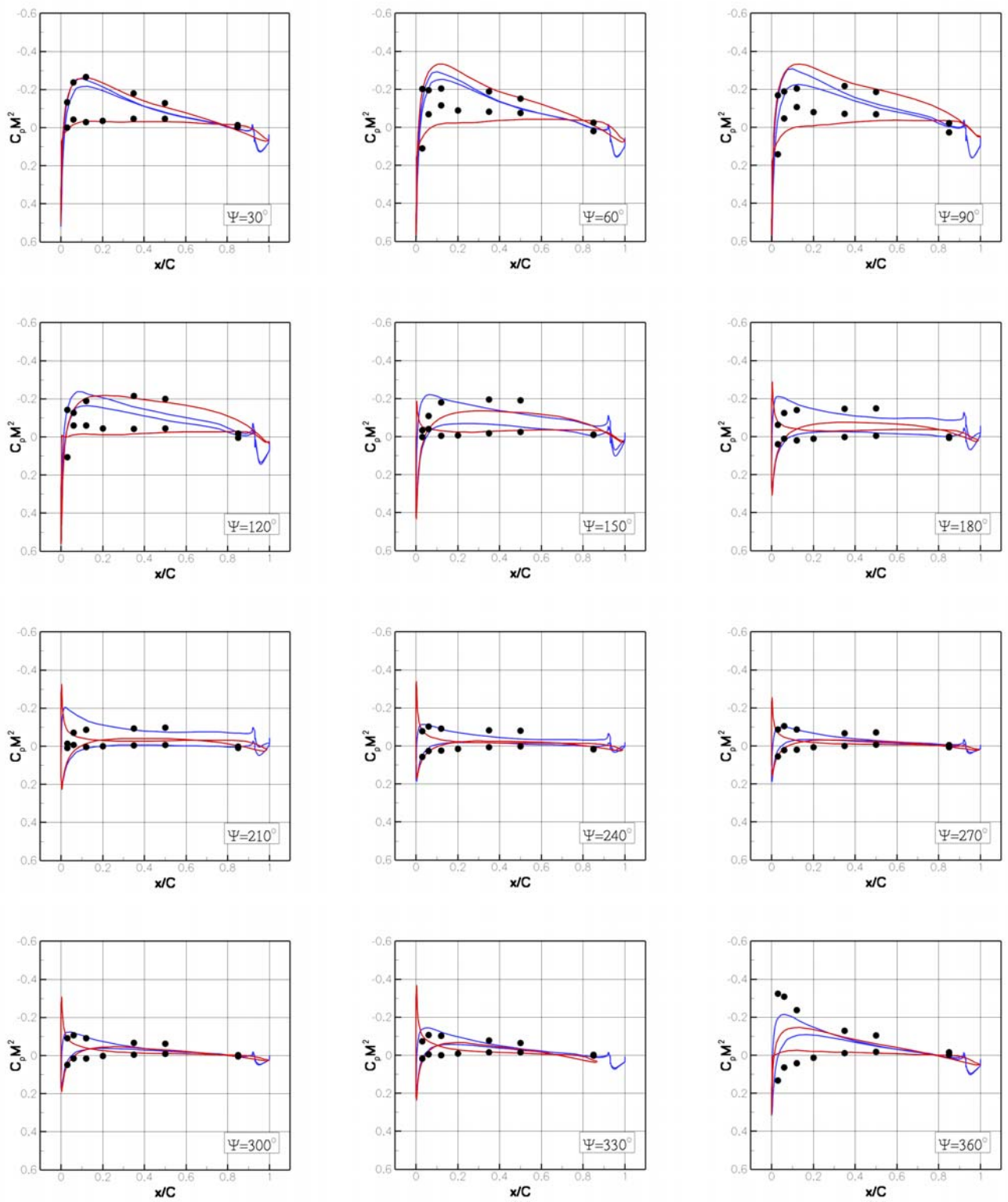
Figure 8: Computed and measured tail rotor sectional pressure at r/R=0.97 at for a complete revolution. Red curves: DLR. Blue curves: PoliMi. Symbols: experiment.